

Gradient-Flowed Thermal Correlators: How Much Flow is Too Much?

Alexander M. Eller, Guy D. Moore

*Institut für Kernphysik, Technische Universität Darmstadt
Schlossgartenstraße 2, D-64289 Darmstadt, Germany*

E-mail: meller@theorie.i kp.physik.tu-darmstadt.de,
guy.moore@physik.tu-darmstadt.de

ABSTRACT: Gradient flow has been proposed in the lattice community as a tool to reduce the sensitivity of operator correlation functions to noisy UV fluctuations. We test perturbatively under what conditions doing so may contaminate the results. To do so, we compute gradient-flowed electric field two-point correlators and stress tensor one- and two-point correlators at finite temperature in QCD. Gradient flow has almost no influence on the value of correlators until a (temperature- and separation-dependent) level of flow is reached, after which the correlator is rapidly compromised. We provide a prescription for how much flow is “safe.”

Contents

1	Introduction	1
2	Gradient flow at temperature in coordinate space	3
3	Calculations	5
3.1	Energy-Momentum Tensor One-Point Function	5
3.2	Electric-Field Correlation Function at Finite Temperature	6
3.3	Stress Tensor Two-Point Functions	9
4	Discussion and conclusions	13

1 Introduction

Gradient flow [1–9] is a nonperturbative and gauge-invariant method in quantum field theory for defining not-quite-local operators with greatly improved insensitivity to ultraviolet fluctuations. Gradient flow is defined by introducing a procedure which, configuration by configuration within the Euclidean path integral, applies “heat equation” evolution to the fields, before constructing operators out of them. Roughly speaking, one can think of this as replacing the fields in an operator with those averaged over a Gaussian envelope. However, by using a nonlinear and gauge-invariant version of the heat equation, the procedure maintains gauge invariance. One can make a rigorous connection between operators under gradient flow and renormalized operators, and all perturbation theory tools needed to study gradient-flowed operators have been developed [5].

The main applications of gradient flow have been within lattice quantum field theory. The value of the F^2 operator ($F^{\mu\nu}$ the field strength) as a function of scale can be used to “read off” the scale-dependent coupling constant and therefore to perform scale setting [7]. Gradient flow is also now widely used to remove UV fluctuations which contaminate the determination of topology on the lattice [10–16]. This is similar to older “smearing” methods [17], with the difference that the gradient-flow approach is on more solid field theoretical foundations.

Gradient flow has also seen its first applications to the study of thermodynamical properties of finite-temperature systems. The energy density and pressure of SU(3) gauge theory were calculated directly on the lattice using gradient flow [18]. This was recently expanded to the energy-momentum tensor in order to determine the equation of state for SU(3) gauge theory [19]. The great advantage of gradient flow in this context is that, by reducing sensitivity to ultraviolet fluctuations, it can dramatically reduce statistical fluctuations in evaluating thermal operator expectation values and correlation functions. For instance, consider

the determination of thermodynamical information. One could evaluate the energy density at temperature by evaluating the difference $\langle T^{00} \rangle_\beta - \langle T^{00} \rangle_{\text{vac}}$, the thermal-to-vacuum difference in the 00 component of the stress tensor. The configuration-by-configuration squared fluctuations in this quantity are set by the 2-point function $\lim_{x \rightarrow 0} \langle T^{00}(x) T^{00}(0) \rangle$. Based on operator dimension, we see that this quantity diverges at small x as x^{-8} . Of course on the lattice this divergence is cut off by the lattice spacing and is $\mathcal{O}(a^{-8})$. This squared fluctuation must be compared to β^{-8} , the square of the size of the energy density difference; the number of spacetime points times configurations must compensate this large ratio to obtain a statistically significant measurement. On the other hand, under gradient flow to a depth τ_F , we expect the overlapping 2-point function to be $\mathcal{O}(\tau_F^{-4})$ (τ_F has dimensions of length^2 , not length). Therefore the UV fluctuations which inhibit a statistically significant evaluation are ameliorated and the number of configurations we must evaluate to obtain good statistics is reduced by a factor¹ of $(a^2/\tau_F)^2$.

A little gradient flow is certainly a good thing, improving statistics, fixing some operator renormalization issues [3], and making the lattice more continuum-like. However, too much gradient flow is definitely bad, as eventually we erase the fluctuations responsible for the physics we want to study. In particular, we want to know, for the study of thermal one-operator and multi-operator correlators, exactly how much gradient flow one may apply before one changes the physics of interest. In this note we will study this problem perturbatively. To our knowledge this is the first perturbative study of thermal correlation functions, and of correlators of spacetime-separated operators, under gradient flow. Therefore we will content ourselves for the moment with a leading-order perturbative evaluation. It is possible that interactions reveal some new physics which makes the situation worse than what we find here, so it would be valuable to extend these calculations to the loop level. However we will leave this for future work.

Here we will consider three types of correlation functions. First and simplest, we consider the stress tensor one-point function at finite temperature. As discussed above, this can be used to measure rather directly the energy density as a function of temperature (if the operator renormalization issues can be resolved; so far the renormalization of a gradient-flowed stress tensor has only been studied perturbatively [5, 8], while a nonperturbative treatment is probably necessary). Second, we will consider the correlator of two electric field operators, embedded along a Polyakov line:

$$G^{\text{EE}}(\tau) = \frac{\langle \text{Re Tr } U(\beta, 0; \tau, 0) E_i(\tau, 0) U(\tau, 0; 0, 0) E_i(0, 0) \rangle}{\langle \text{Re Tr } U(\beta, 0; 0, 0) \rangle} \quad (1.1)$$

where $U(t_1, x_1; t_2, x_2)$ is a straight Wilson line from point (t_1, x_1) to point (t_2, x_2) and E_i is the electric field. This operator was introduced in [20], who show that its analytical continuation to Minkowski frequency determines the (momentum-space and coordinate-space) diffusion of a heavy quark, $m_q \gg T$ in a thermal bath. Recently there has been a vigorous effort to measure this correlation function on the lattice [21], but so far only quenched results are available and the issue of the E -field renormalization has not been resolved.

¹The factor is $(a^2/\tau_F)^2$ and not $(a^2/\tau_F)^4$ because there is only one independent measurement per τ_F^2 of volume, rather than every a^4 of volume.

Gradient flow would fix the renormalization issue and will hopefully improve statistical power such that the correlation function can be reliably measured at the nonperturbative level. Finally, we will consider the correlation function of two stress tensors at vanishing spatial momentum (equivalently, integrated over spatial separation) as a function of the Euclidean time separation τ . For those $T^{\mu\nu}$ components which couple to hydrodynamical modes, such as $T^{00}T^{00}$ and $T^{0i}T^{0i}$, the correlator should be τ -independent and should reproduce thermodynamical information (the heat conductivity and enthalpy density respectively). For the $\ell = 2$ space component, e.g. $T^{xy}T^{xy}$, the analytical continuation of the correlator holds information about the shear viscosity [22–25].

In the next section we will develop perturbative tools for gradient flow at finite temperature in coordinate space, which turns out to be the most convenient for the problems we study here. Next, Section 3 contains the specific details of the leading-order calculations of each correlator mentioned above. In every case we find that there is a (τ -dependent) range of flow times τ_F for which the correlator feels exponentially suppressed corrections; but for more flow it quickly goes wrong. We end with a discussion which presents our recommendations for the amount of flow which can be applied “safely,” given our lowest-order perturbative results.

2 Gradient flow at temperature in coordinate space

We write the unflowed gauge field as $A_\mu^a(x)$ and will generally suppress the color index a . The flowed gauge field $B_\mu(x, \tau_F)$ is defined at nonnegative flow time τ_F through the $\tau_F = 0$ boundary condition

$$B_\mu(x, \tau_F)|_{\tau_F=0} = A_\mu(x) \quad (2.1)$$

and the flow equation

$$\frac{\partial B_\mu(x, \tau_F)}{\partial \tau_F} = D_\nu G_{\nu\mu}(x, \tau_F) + \alpha_0 D_\mu \partial_\nu B_\nu(x, \tau_F), \quad (2.2)$$

where $G_{\nu\mu}(x, \tau_F)$ is the field strength tensor written using $B_\mu(x, \tau_F)$ rather than $A_\mu(x)$. The second term in the flow equation constitutes as τ_F -dependent gauge choice, which is convenient to make in the context of perturbative calculations [3]. Choosing $\alpha_0 = 1$ and working to linearized order, the flow equation simplifies to

$$\frac{\partial B_\mu(x, \tau_F)}{\partial \tau_F} = \partial_\nu \partial_\nu B_\mu(x, \tau_F), \quad (2.3)$$

which is the heat equation.

In vacuum, the Feynman-gauge momentum-space propagator after flow is

$$G_E^{BB}(p, \tau_{F1}, \tau_{F2}) = \int d^4x e^{ip_\mu x^\mu} \langle B_\mu(x, \tau_{F1}) B_\nu(0, \tau_{F2}) \rangle = g^2 \delta_{\mu\nu} \frac{e^{-(\tau_{F1} + \tau_{F2})p^2}}{p^2} \quad (2.4)$$

and Fourier transforming leads to the zero temperature flowed propagator in coordinate space

$$G_E^{BB}(x, \tau_{F1}, \tau_{F2}) = \frac{g^2 \delta_{\mu\nu}}{4\pi^2 x^2} \left(1 - e^{-\frac{x^2}{4(\tau_{F1} + \tau_{F2})}} \right). \quad (2.5)$$

This result was found by Lüscher in [3]. But we could have reached this result faster by noting that the coordinate-space propagator before flow is the solution to the Poisson equation $-\partial_\mu^2 G_E^{AA}(x) = g^2 \delta^4(x)$, which is $G_E^{AA}(x) = g^2/(4\pi^2 x^2)$. At tree level and in Feynman gauge, flow is the application of the heat equation to this propagator, which is the same as convolving it with a Gaussian envelope,

$$G^{BB}(x, \tau_{F_1}, \tau_{F_2}) = \int d^4 y \frac{g^2}{4\pi^2 y^2} e^{-\frac{(x-y)^2}{4(\tau_{F_1} + \tau_{F_2})}} = \frac{g^2}{4\pi^2 x^2} \left(1 - e^{-\frac{x^2}{4(\tau_{F_1} + \tau_{F_2})}} \right). \quad (2.6)$$

Alternatively, one may take the right-hand expression as an *Ansatz* and verify that it satisfies the $\tau_F = 0$ boundary conditions and the heat equation.

To introduce finite temperature, we restrict the Euclidean time to lie in $x^0 \in [0, \beta]$ with periodic boundary conditions. The fast way to find the coordinate-space propagator is to note that the Poisson equation is now solved using the method of images;

$$G_{E,\beta}^{AA}(x^0, \vec{x}) = \sum_{n \in \mathbb{Z}} \frac{g^2}{4\pi^2 x_n^2}, \quad x_n^\mu \equiv (x^0 + n\beta, \vec{x}), \quad (2.7)$$

and that flow again corresponds to evolving this propagator under the heat equation or convolving with a Gaussian:

$$G_{E,\beta}^{BB}(x, \tau_{F_1}, \tau_{F_2}) = \sum_{n=-\infty}^{\infty} \frac{g^2 \delta_{\mu\nu}}{4\pi^2 x_n^2} \left(1 - e^{-\frac{x_n^2}{4(\tau_{F_1} + \tau_{F_2})}} \right). \quad (2.8)$$

We could also arrive at this result the “hard way” by Fourier transforming the finite-temperature, flowed momentum-space propagator

$$G_E^{BB}(x, \tau_{F_1}, \tau_{F_2}) = T \sum_{p^0=2\pi mT}^{m \in \mathbb{Z}} \int \frac{d^3 p}{(2\pi)^3} e^{ip \cdot x} \times \frac{g^2 e^{-p^2(\tau_{F_1} + \tau_{F_2})}}{p^2} \quad (2.9)$$

by use of Poisson’s summation formula [26]

$$T \sum_{p^0=2\pi mT}^{m \in \mathbb{Z}} = \sum_{n \in \mathbb{Z}} \int_{-\infty}^{\infty} \frac{dp^0}{2\pi} e^{ip^0 \beta n} \quad (2.10)$$

to rewrite the summation over p^0 as a sum over coordinate-space copies – essentially, the same images as above. At this point each $\int dp^0$ term represents a vacuum contribution with a different x^0 position, shifted into one of the image copies. This leads rather directly back to Eq. (2.8). In the following we will only work at finite temperature so we will suppress the subscript β .

When we take correlation functions, we will have to include a sum over images for *each* propagator which appears. We present a cartoon of this procedure in Figure 1.

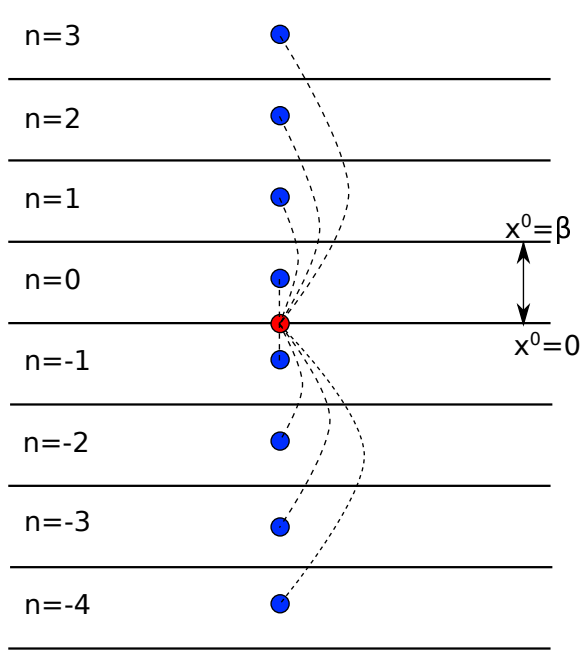


Figure 1. Cartoon of the images and correlation of the finite-temperature gauge-field propagator. The colored circles represent the gauge fields, the horizontal lines the periodic boundaries in the time plane, and the dashed lines the correlations between one field and the images of the other.

3 Calculations

We will now use the coordinate-space propagator to compute the desired correlation functions. While the last section has introduced propagators between fields with different amounts of flow, here we will only consider correlators where all operators are evaluated after the same amount of flow τ_F ; so the previous formulae should be modified by writing $\tau_{F1} = \tau_{F2} = \tau_F$.

3.1 Energy-Momentum Tensor One-Point Function

The tree-level energy-momentum tensor in Yang-Mills theory is²

$$T_{\mu\nu}^B(x, \tau_F) = \frac{1}{g^2} \left[(G_{\mu\sigma}^a G_{\nu\sigma}^a)(x, \tau_F) - \frac{1}{4} \delta_{\mu\nu} (G_{\omega\sigma}^a G_{\omega\sigma}^a)(x, \tau_F) \right], \quad (3.1)$$

$$G_{\mu\nu}(x, \tau_F) = \partial_\mu^x B_\nu(x, \tau_F) - \partial_\nu^x B_\mu(x, \tau_F).$$

We evaluate the correlator of two field strengths by splitting the field strengths to reside at points x, y , write

$$\langle B_\mu(x, \tau_F) B_\nu(y, \tau_F) \rangle = G_E^{BB}(x - y, \tau_F) \quad (3.2)$$

which we found in Eq. (2.8), take derivatives, and then set $x = y$. Introducing a dimensionless rescaled flow time $\tilde{\tau}_F \equiv 8\tau_F/\beta^2$, we evaluate the two field strength correlators which

²At the loop level we would need to include the trace anomaly.

we need,

$$\langle G_{0\sigma}^a G_{0\sigma}^a \rangle = \frac{3g^2 d_A}{\pi^2 \beta^4} \sum_{n \in \mathcal{Z}} \left[e^{-\frac{n^2}{\tilde{\tau}_F}} \cdot \left(\frac{1}{\tilde{\tau}_F^2} + \frac{1}{\tilde{\tau}_F} \frac{1}{n^2} + \frac{1}{n^4} \right) - \frac{1}{n^4} \right], \quad (3.3)$$

$$\langle G_{i\sigma}^a G_{i\sigma}^a \rangle = \frac{3g^2 d_A}{\pi^2 \beta^4} \sum_{n \in \mathcal{Z}} \left[e^{-\frac{n^2}{\tilde{\tau}_F}} \cdot \left(\frac{1}{\tilde{\tau}_F^2} - \frac{1}{\tilde{\tau}_F} \frac{1}{n^2} - \frac{1}{n^4} \right) + \frac{1}{n^4} \right], \quad (3.4)$$

where each n^2 arises as x_n^2/β^2 . Then we combine them to find a closed expression for the stress-tensor one-point function after flow,

$$\langle T_{00} \rangle = -\langle T_{ii} \rangle = \frac{3d_A}{\pi^2 \beta^4} \sum_{n \in \mathcal{Z}} \left[e^{-\frac{n^2}{\tilde{\tau}_F}} \cdot \left(\frac{1}{2\tilde{\tau}_F^2} + \frac{1}{\tilde{\tau}_F} \frac{1}{n^2} + \frac{1}{n^4} \right) - \frac{1}{n^4} \right]. \quad (3.5)$$

Here $d_A = N_c^2 - 1 = 8$ is the dimension of the group, which counts gluon colors. The sum over n is a sum over images; the vacuum result is the $n = 0$ term, which is defined as the $n \rightarrow 0$ limit and which actually vanishes. In the $\tau_F \rightarrow 0$ limit the exponential terms vanish and we have only the $1/n^4$ term, confirming as expected that

$$\langle T_{00} \rangle = -\frac{3d_A}{\pi^2 \beta^4} \sum_{n \neq 0} \frac{1}{n^4} = -\frac{6d_A}{\pi^2 \beta^4} \zeta(4), \quad (3.6)$$

the standard Stefan-Boltzmann result.

In the opposite limit, $\tilde{\tau}_F \gg 1$, many terms contribute to the sum and we may approximate it with an integral, giving rise to

$$\begin{aligned} \langle T_{00} \rangle_\beta &\xrightarrow{\tilde{\tau}_F \gg 1} \frac{3d_A}{\pi^2 \beta^4} \frac{1}{\tilde{\tau}_F^{3/2}} \int_{-\infty}^{\infty} du \frac{1}{u^4} \left[-1 + \left(1 + u^2 + \frac{u^4}{2} \right) e^{-u^2} \right] \\ &= -\frac{3d_A}{\pi^2 \beta^4} \frac{1}{\tilde{\tau}_F^{3/2}} \frac{\sqrt{\pi}}{6} = -\frac{d_A}{32\sqrt{2}\pi^{3/2}\tau_F^{3/2}\beta}. \end{aligned} \quad (3.7)$$

This result corresponds to the contribution arising from the zero Matsubara frequency, as all other Matsubara frequencies are damped away by the flow.

For finite $\tilde{\tau}_F$ we evaluate the sum numerically and display the result in Figure 2. The plot shows that, for small $\tilde{\tau}_F$, the corrections to Stefan-Boltzmann are exponentially small, physically representing the exponentially small amplitude for the “smearing” due to flow to stretch all the way around the periodic direction. However the stability of the result then rather abruptly breaks down above $\tilde{\tau}_F \sim 0.12$, and for large $\tilde{\tau}_F$ values the thermal contribution is almost completely lost. If we require that the flow change the determined energy density by at most 1%, then we can constrain the allowed flow depth to be $8\tau_F/\beta^2 \leq 0.12$. On the lattice with N_t lattice points around the temporal direction, that corresponds to $\tau_F/a^2 \leq 0.015N_t^2$ with a the lattice spacing.

3.2 Electric-Field Correlation Function at Finite Temperature

In Eq. (1.1) we see that the electric field correlator of interest contains Wilson lines forming a Polyakov loop. However in a lowest-order evaluation these are irrelevant, and only

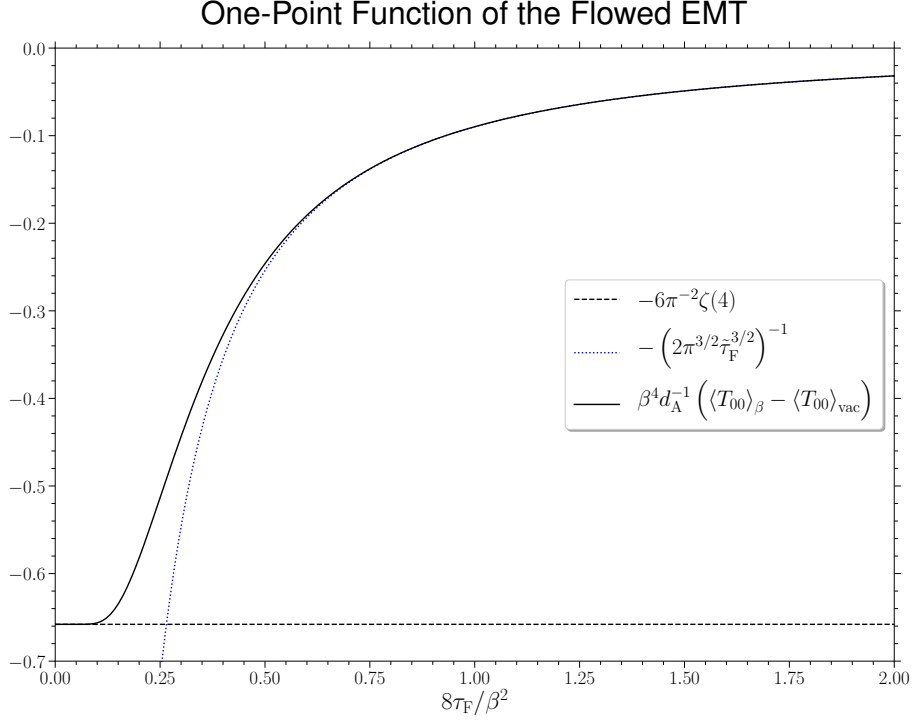


Figure 2. Plot of the one-point function of the energy-momentum tensor as a function of the applied gradient flow, together with its asymptotic small τ_F and large τ_F behavior.

derivatives of the gauge-field propagator are involved. The leading-order contribution reads

$$\left\langle E_i^a(x, \tau_F) E_j^b(0, \tau_F) \right\rangle = \partial_0^x \partial_0^y \left\langle B_i^a(x, \tau_F) B_j^b(y, \tau_F) \right\rangle + \partial_i^x \partial_j^y \left\langle B_0^a(x, \tau_F) B_0^b(y, \tau_F) \right\rangle \Big|_{y=0}. \quad (3.8)$$

Differentiating and introducing the dimensionless scaled coordinate $\tilde{x}_n = x_n/\beta$ and the ratio of squared coordinate to flow time $\tilde{\xi}_n^2 = \tilde{x}_n^2/\tilde{\tau}_F$, we find

$$\begin{aligned} \left\langle E_i^a(x, \tau_F) E_j^b(0, \tau_F) \right\rangle &= \frac{g^2 \delta^{ab}}{\pi^2} \sum_{n \in \mathcal{Z}} \frac{1}{\tilde{x}_n^4} \left[\frac{\delta_{ij} (\tilde{x}_n^0)^2 + \tilde{x}_i \tilde{x}_j}{\tilde{x}_n^2} \left((\tilde{\xi}_n^4 + 2\tilde{\xi}_n^2 + 2) e^{-\tilde{\xi}_n^2} - 2 \right) \right. \\ &\quad \left. + \delta_{ij} \left(1 - (1 + \tilde{\xi}_n^2) e^{-\tilde{\xi}_n^2} \right) \right]. \end{aligned} \quad (3.9)$$

In this expression we have allowed the electric fields to be at different spatial coordinates, but the correlator relevant for heavy quark transport involves $\vec{x} = 0$, which we will set from now on. Our result then simplifies to

$$\left\langle E_i^a(x^0, \tau_F) E_j^b(0, \tau_F) \right\rangle = \frac{g^2 \delta^{ab}}{\pi^2 \beta^4} \sum_{n \in \mathcal{Z}} \frac{\delta_{ij}}{\tilde{x}_n^4} \left[(\tilde{\xi}_n^4 + \tilde{\xi}_n^2 + 1) e^{-\tilde{\xi}_n^2} - 1 \right]. \quad (3.10)$$

This is the main result of this section.

To explore this result further, we consider first the limit of small flow time, $\tilde{\tau}_F \rightarrow 0$ or $\tilde{\xi} \rightarrow \infty$. In this limit $(\tilde{\xi}^4 + \tilde{\xi}^2 + 1) e^{-\tilde{\xi}^2} \simeq 0$. The sum can be performed analytically and

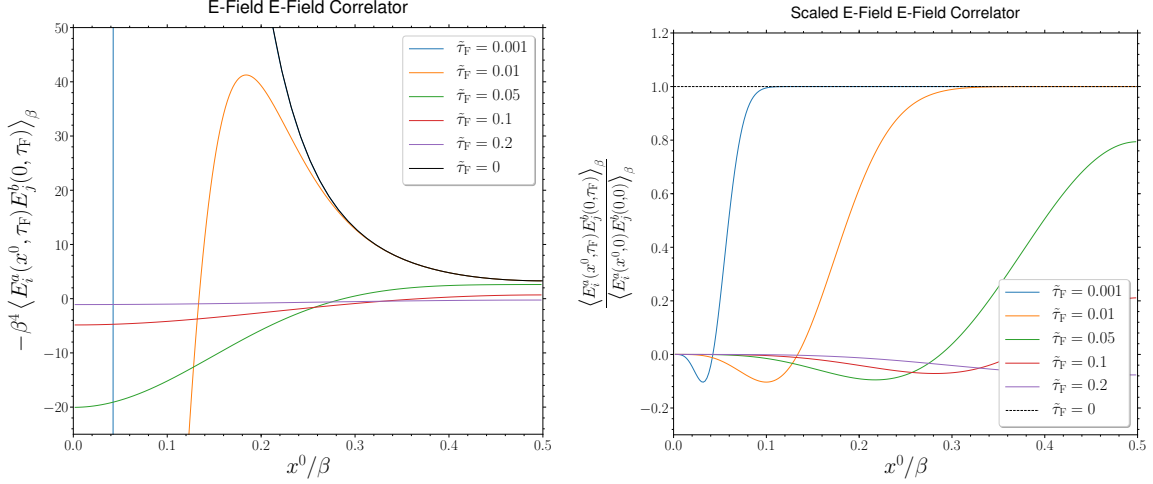


Figure 3. Left: plot of the free-theory electric-field electric-field correlation, Right: the same, normalized to the unflowed behavior

the result is

$$\langle E_i^a(x, \tau_F) E_j^b(0, \tau_F) \rangle = -\frac{\pi^2 g^2 \delta^{ab} \delta_{ij} \cos(2\pi \tilde{x}^0) + 2}{\beta^4 3 \sin^4(\pi \tilde{x}^0)}. \quad (3.11)$$

The correlation function is negative, as expected; the electric field is odd under the time-reflection operator

$$E \xrightarrow{\Theta} -E, \quad (3.12)$$

and so its correlation function should be negative. Note however that the time-integrated $\langle EE \rangle$ correlator could still be positive due to contact terms when the operators overlap.

We can also explore the opposite limit of large flow time, $\tilde{\tau}_F \gg 1$, which allows us to approximate the sum over n with an integral,

$$\begin{aligned} \langle E_i^a(x, \tau_F) E_j^b(0, \tau_F) \rangle &\xrightarrow{\tilde{\tau}_F \gg 1} \frac{g^2 \delta^{ab}}{\pi^2 \beta^4} \int_{-\infty}^{\infty} dn \frac{\delta_{ij}}{\tilde{x}_n^4} \left[(\tilde{\xi}_n^4 + \tilde{\xi}_n^2 + 1) e^{-\tilde{\xi}_n^2} - 1 \right] \\ &= \frac{g^2 \delta^{ab}}{\pi^2} \frac{\delta_{ij}}{\beta^4 \tilde{\tau}_F^{3/2}} \int_{-\infty}^{\infty} du \frac{1}{u^4} \left[-1 + (1 + u^2 + u^4) e^{-u^2} \right] \\ &= \frac{g^2 \delta^{ab} \delta_{ij}}{48 \sqrt{2} \pi^{3/2} \tau_F^{3/2} \beta}, \end{aligned} \quad (3.13)$$

which is the same result we would get by considering only the contribution of the zero Matsubara frequency. In contrast to the small $\tilde{\tau}_F$ limit, this result is positive. There is no contradiction with fundamental theorems, because the operator after flow is no longer local, so Θ -odd behavior does not ensure negative correlations. But this indicates that the result at large flow times has been thoroughly contaminated with contact-term type contributions. Once a correlator which is expected to be negative becomes positive due to flow, the character of the correlation function has been fundamentally altered.

The sum in Eq. (3.10) can be evaluated numerically. In Figure 3, the behavior of the correlator is shown for different values of $\tilde{\tau}_F$. The black curve is the analytic result for

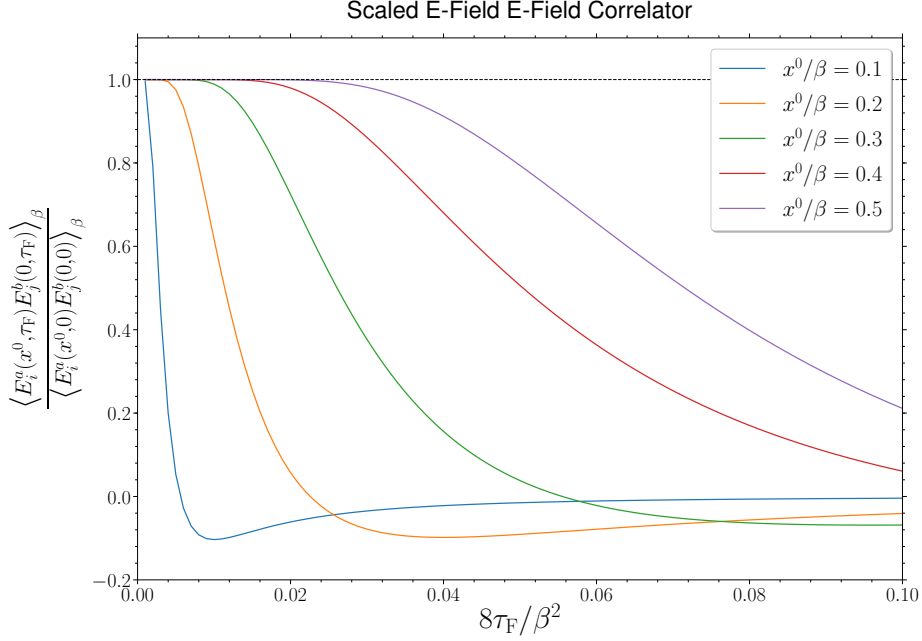


Figure 4. Plot of the electric-field electric-field correlator normalized to the unflowed behavior at fixed time separations as a function of flow times.

zero flow from Eq. (3.10). The blue curve related to a flow time of $\tilde{\tau}_F = 0.001$ is hidden under the zero flow curve for $x^0/\beta > 0.2$. Figure 3 shows that as we increase the amount of flow, the x^0 range for which the correlator remains almost unchanged gets narrower; for the larger flow times shown, the two never coincide. Therefore the amount of flow which we can “get away with” is x^0 dependent, which should not be too surprising.

It is also instructive to explore the correlator as a function of flow time at fixed separation. Figure 4 shows a plot of this function. The behavior of the function is exactly as expected. For small flow times, the correlator shows a plateau of the unflowed value and the amount of flow which damages the correlator depends on the separation. If we use more flow, the correlator changes sign. For enough flow it becomes small as all fluctuations are damped away.

In Table 3.2 we show the maximum amount of flow before the correlator changes by 1% as a function of x^0 . We believe that this can be used as a criterion for how much flow one can “get away with” in measuring the EE correlator at a given x^0 value.

3.3 Stress Tensor Two-Point Functions

The calculation of the stress tensor two-point correlator is similar to the electric field correlator, except that each stress tensor contains two field strengths. Since there are two gauge field propagators, there is now a double sum over images. The connected stress

Table 1. List of the flow times needed to change the $\langle EE \rangle$ correlator by 1% relative to the zero-flow value, for different x^0 separations.

$\frac{x^0}{\beta}$	$\frac{8\tau_F}{\beta^2}$
0.1	0.0011
0.2	0.0044
0.3	0.0099
0.4	0.0180
0.5	0.0274

tensor two-point function is

$$\begin{aligned}
& \langle G_{\mu\sigma} G_{\nu\sigma}(x, \tau_F) G_{\alpha\omega} G_{\beta\omega}(0, \tau_F) \rangle \\
&= \frac{dAg^4}{16\pi^4} C_{\mu\nu\alpha\beta, abcdefgh} \partial_a^x \partial_b^{x'} \partial_c^y \partial_d^{y'} \\
&\times \left\{ \left[\sum_n \frac{\delta_{eg}}{(x-y)_n^2} \left(1 - e^{-\frac{(x-y)_n^2}{8\tau_F}} \right) \right] \left[\sum_m \frac{\delta_{fh}}{(x'-y')_m^2} \left(1 - e^{-\frac{(x'-y')_m^2}{8\tau_F}} \right) \right] \right. \\
&\quad \left. + \left[\sum_n \frac{\delta_{eh}}{(x-y')_n^2} \left(1 - e^{-\frac{(x-y')_n^2}{8\tau_F}} \right) \right] \left[\sum_m \frac{\delta_{fg}}{(x'-y)_m^2} \left(1 - e^{-\frac{(x'-y)_m^2}{8\tau_F}} \right) \right] \right\} \Big|_{x=x', y=y'=0}, \tag{3.14}
\end{aligned}$$

where we have introduced the Lorentz structure

$$C_{\mu\nu\alpha\beta, abcdefgh} = (\delta_{\mu a} \delta_{\sigma e} - \delta_{\mu e} \delta_{\sigma a}) (\delta_{\nu b} \delta_{\sigma f} - \delta_{\nu f} \delta_{\sigma b}) (\delta_{\alpha c} \delta_{\omega g} - \delta_{\alpha g} \delta_{\omega c}) (\delta_{\beta d} \delta_{\omega h} - \delta_{\beta h} \delta_{\omega d}). \tag{3.15}$$

The derivatives can be applied for each sum separately,

$$\partial_a^x \partial_c^y \frac{\delta_{eg}}{(x-y)_n^2} \left(1 - e^{-\frac{(x-y)_n^2}{8\tau_F}} \right) \Big|_{y=0} = \frac{4\delta_{eg}}{\pi^2 x_n^4} \left(\delta_{ac} A_n(x, \tau_F) + \frac{x_{na} x_{nc}}{x_n^2} B_n(x, \tau_F) \right) \tag{3.16}$$

with the dimensionless scalar functions defined as

$$A_n(x, \tau_F) = \frac{1}{2} \left(1 - (1 + \tilde{\xi}_n^2) e^{-\tilde{\xi}_n^2} \right), \tag{3.17}$$

$$B_n(x, \tau_F) = -2 + \left(2 + 2\tilde{\xi}_n^2 + \tilde{\xi}_n^4 \right) e^{-\tilde{\xi}_n^2}. \tag{3.18}$$

Because at leading order $T_{00} = -T_{ii}$, there are three independent stress-tensor correlators (at vanishing spatial momentum) for which we can apply these formulae,

$$\langle T_{00} T_{00} \rangle_\beta, \quad \langle T_{0i} T_{0i} \rangle_\beta, \quad \langle (T_{ij} - \frac{1}{3} \delta_{ij} T_{kk}) (T_{ij} - \frac{1}{3} \delta_{ij} T_{ll}) \rangle \equiv \langle T_{ij}^{\text{tr}} T_{ij}^{\text{tr}} \rangle, \tag{3.19}$$

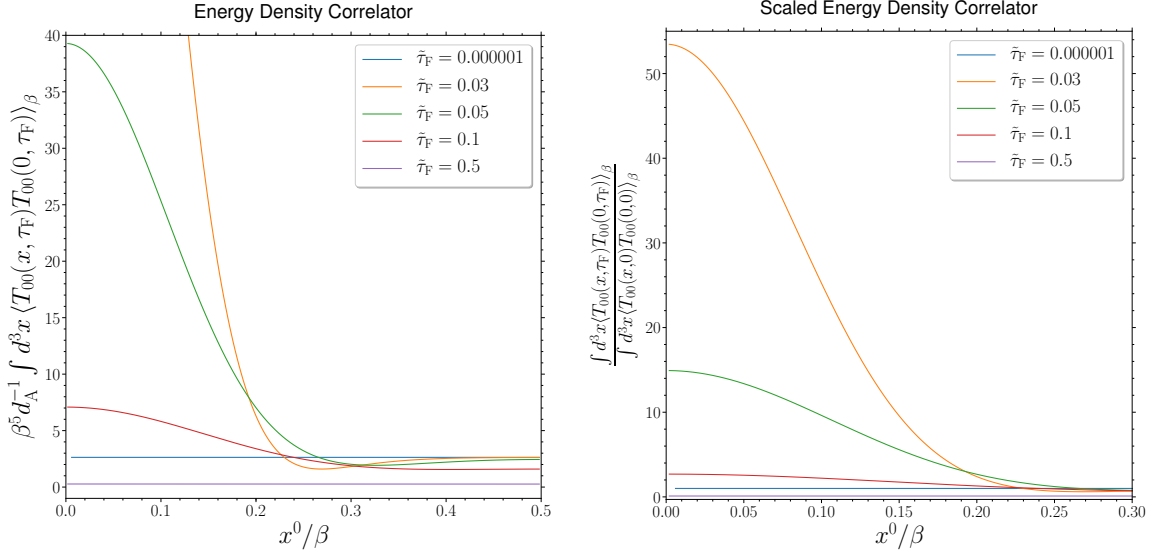


Figure 5. Plot of the $\langle T_{00}T_{00} \rangle$ correlator at zero spatial momentum as a function of temporal separation, for selected values of flow time.

which evaluate to

$$\langle T_{00}(x, \tau_F) T_{00}(0, \tau_F) \rangle = \frac{d_A}{\pi^4} \sum_n \sum_m \left[12 \frac{A_n A_m}{x_n^4 x_m^4} + 3 \frac{(A_n B_m + A_m B_n)}{x_n^4 x_m^4} \right] \quad (3.20)$$

$$+ \left((x_n \cdot x_m)^2 + \frac{1}{2} x_n^2 x_m^2 - 4 \tilde{x}^2 x_{n,0} x_{m,0} \right) \frac{B_n B_m}{x_n^6 x_m^6} \Big],$$

$$\langle T_{0i}(x, \tau_F) T_{0i}(0, \tau_F) \rangle = \frac{d_A}{\pi^4} \sum_n \sum_m \left[24 \frac{A_n A_m}{x_n^4 x_m^4} + 6 \frac{(A_n B_m + A_m B_n)}{x_n^4 x_m^4} \right] \quad (3.21)$$

$$+ \left((x_n \cdot x_m)^2 + 4 x_{n,0}^2 \tilde{x}^2 - x_{n,0}^2 x_{m,0}^2 + \tilde{x}^4 \right) \frac{B_n B_m}{x_n^6 x_m^6} \Big],$$

$$\langle T_{ij}^{\text{tr}}(x, \tau_F) T_{ij}^{\text{tr}}(0, \tau_F) \rangle = \frac{d_A}{\pi^4} \sum_n \sum_m \left[80 \frac{A_n A_m}{x_n^4 x_m^4} + 20 \frac{(A_n B_m + A_m B_n)}{x_n^4 x_m^4} \right] \quad (3.22)$$

$$+ \left(10 (x_n \cdot x_m)^2 - \frac{52}{3} (x_n \cdot x_m) \tilde{x}^2 + \frac{10}{3} (x_n^2 + x_m^2) \tilde{x}^2 + \frac{2}{3} \tilde{x}^4 \right) \frac{B_n B_m}{x_n^6 x_m^6} \Big].$$

These are the main analytic results of this section.

We are interested in the $\vec{p} = 0$ channel and thus need to integrate over $\int d^3x$. At this point we resort to a numerical evaluation. In Figure 5 the results for the energy density–energy density component $\langle T_{00}T_{00} \rangle$ are shown. Energy conservation implies that for vanishing flow time the correlator should be a flat line at a value set by the heat capacity, which in the free theory is $\frac{4\pi^2 d_A}{15\beta^5}$. Such consequences of stress conservation hold up to exponentially small corrections so long as $\tilde{\xi}^2 \gg 1$. However, for larger flow extents, operators effectively overlap, and contact terms contaminate consequences of stress conservation. Therefore, when the flow depth approaches the squared separation, the constancy

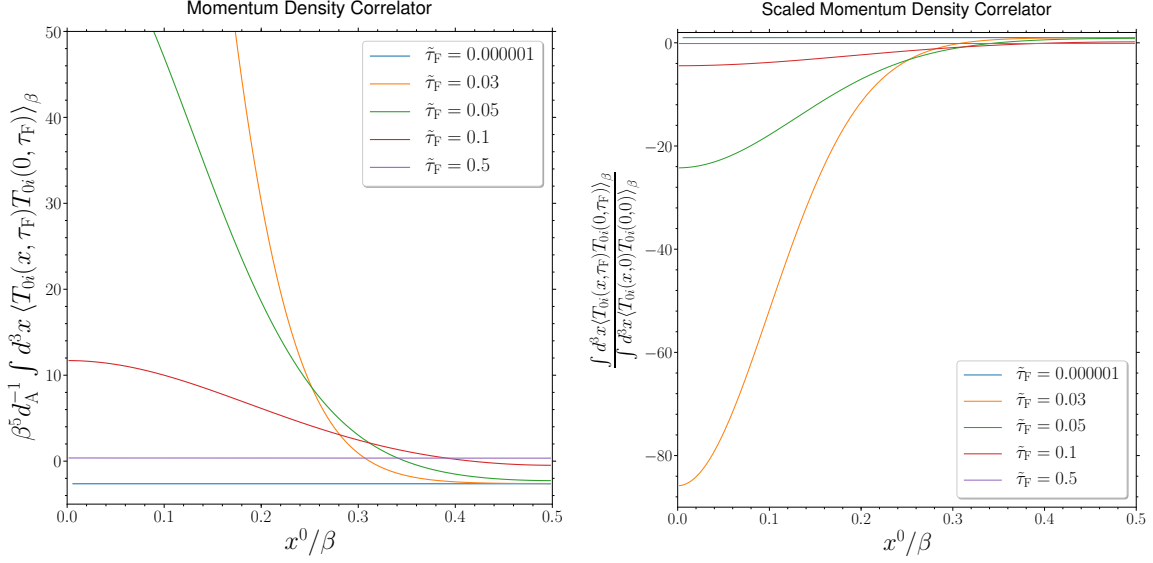


Figure 6. Momentum density correlator as a function of temporal separation at selected flow depths.

of the correlator will be lost. This is indeed what we observe. For large values of flow time $\tilde{\tau}_F \gg 1$, the correlator becomes flat again, as it is dominated by the time-independent zero Matsubara frequency contribution.

The momentum–momentum component $\langle T_{0i} T_{0i} \rangle$ is related to momentum fluctuations in the medium. Without flow, it should be constant and negative, with value set by the enthalpy density times temperature, $\frac{4\pi^2 d_A}{15\beta^5}$. The behavior under flow is shown in Figure 6. The flow time dependence is similar to that for the $\langle T_{00} T_{00} \rangle$ correlator, for the same physical reasons.

The stress–stress component $\left\langle \left(T_{ij} - \frac{1}{3} \delta_{ij} T_{ll} \right) \left(T_{ij} - \frac{1}{3} \delta_{ij} T_{kk} \right) \right\rangle$ is physically interesting because its continuation to a spectral function determines the shear viscosity [22–25]. Because it is not constrained by conservation laws, no short-distance cancellations occur and it shows strong short-distance divergent behavior; the unflowed behavior is dominated by the vacuum contribution which diverges at the origin. If we use gradient flow, the correlator is finite at the origin and for intermediate flow times $0.01 < \tilde{\tau}_F < 0.1$ we find a non-trivial behavior. The numerical results are presented in Figure 7. For large flow times the zero Matsubara frequency again dominates the correlator, which is nearly x^0 independent.

The main result of this numerical evaluation is that if we are using flow to suppress fluctuations in our correlators, then the $\langle T_{00} T_{00} \rangle$ and $\langle T_{0i} T_{0i} \rangle$ correlators are best evaluated at $x^0 = \beta/2$ and with at most $8\tau_F/\beta^2 < 0.027$. For $\langle T_{ij} T_{ij} \rangle$ one should use the same τ_F values as for the electric field correlator with the same x^0 value.

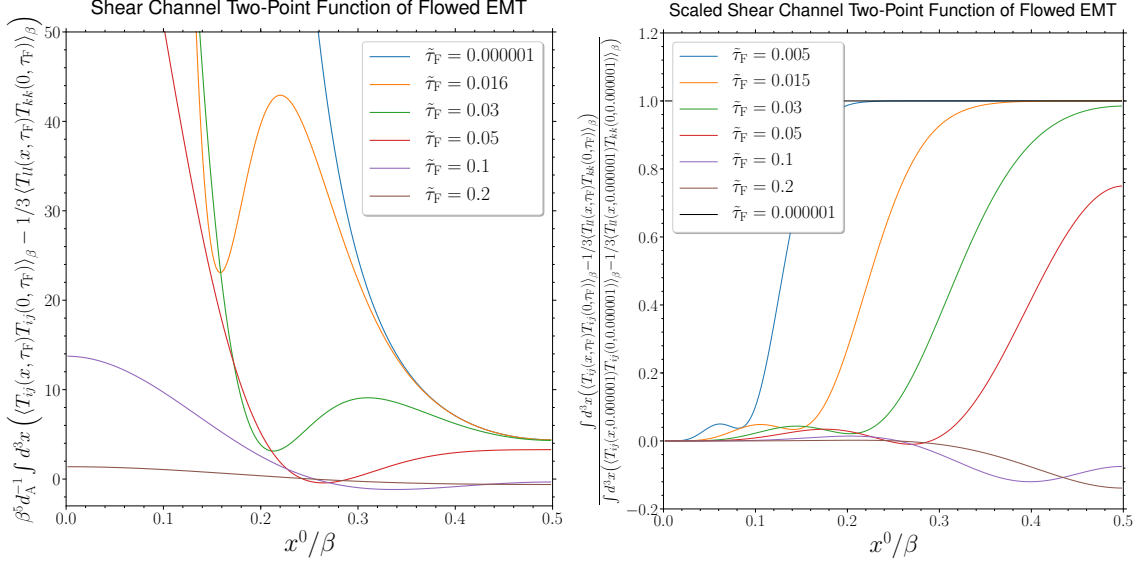


Figure 7. Left: plot of the shear channel two-point function of the energy-momentum tensor as a function of temporal separation. Right: the same but normalized to the unflowed result.

4 Discussion and conclusions

Gradient flow successfully reduces short-distance fluctuations, which is a boon for reducing statistical fluctuations in the lattice determination of local operator correlation functions. Therefore there is an interest in applying it to lattice measurements of correlation functions. Here we made a first exploration of how reliable this approach may be at finite temperature, for the evaluation of the energy density T_{00} and of electric field and stress tensor two-point functions. At lowest order in perturbation theory, we found that the energy density of the thermal bath is obtained reliably provided that the flow depth obeys $\tau_F < 0.015\beta^2$ (or $\tau_F/a^2 = 0.015N_t^2$ on the lattice), whereas a 2-point function of field strengths or stress tensors separated by a distance x^0 is reproduced reliably for $\tau_F < 0.014(x^0)^2$ (or $\tau_F/a^2 = 0.014(\Delta N_t)^2$ on the lattice, where ΔN_t is the minimum number of lattice units of separation between the two operators to be evaluated). Exceeding this amount of flow causes contact-term contamination in the correlator, either between operators or between an operator and its periodic images. However, below this amount of flow, the effect of flow on the correlation function due to these effects is exponentially small, and consequences of symmetries such as stress tensor conservation are preserved up to exponential corrections.

It would be valuable to extend this study to the loop level, to see how operator renormalization, the Wilson line appearing in the definition of the electric field two-point function, and other interaction effects enter, and to check whether these effects modify our conclusions.

Acknowledgments

We thank the Technische Universität Darmstadt and its Institut für Kernphysik, where this work was conducted. This work was supported by the Deutsche Forschungsgemeinschaft (DFG) through the grant CRC-TR 211 “Strong-interaction matter under extreme conditions.”

References

- [1] R. Narayanan and H. Neuberger. Infinite N phase transitions in continuum Wilson loop operators. *JHEP*, 03:064, 2006.
- [2] Martin Lüscher. Trivializing maps, the Wilson flow and the HMC algorithm. *Commun. Math. Phys.*, 293:899–919, 2010.
- [3] Martin Lüscher. Properties and uses of the Wilson flow in lattice QCD. *JHEP*, 08:071, 2010. [Erratum: JHEP03,092(2014)].
- [4] Martin Lüscher. Topology, the Wilson flow and the HMC algorithm. *PoS, LATTICE2010:015*, 2010.
- [5] Martin Lüscher and Peter Weisz. Perturbative analysis of the gradient flow in non-abelian gauge theories. *JHEP*, 02:051, 2011.
- [6] Hiroshi Suzuki. Energymomentum tensor from the YangMills gradient flow. *PTEP*, 2013:083B03, 2013. [Erratum: PTEP2015,079201(2015)].
- [7] Martin Lüscher. Future applications of the Yang-Mills gradient flow in lattice QCD. *PoS, LATTICE2013:016*, 2014.
- [8] Kenji Hieda, Hiroki Makino, and Hiroshi Suzuki. Proof of the renormalizability of the gradient flow. *Nucl. Phys.*, B918:23–51, 2017.
- [9] Hiroshi Suzuki. Energy–momentum tensor on the lattice: recent developments. *PoS, LATTICE2016:002*, 2017.
- [10] Evan Berkowitz, Michael I. Buchoff, and Enrico Rinaldi. Lattice QCD input for axion cosmology. *Phys. Rev.*, D92(3):034507, 2015.
- [11] S. Borsanyi, M. Dierigl, Z. Fodor, S. D. Katz, S. W. Mages, D. Nogradi, J. Redondo, A. Ringwald, and K. K. Szabo. Axion cosmology, lattice QCD and the dilute instanton gas. *Phys. Lett.*, B752:175–181, 2016.
- [12] Peter Petreczky, Hans-Peter Schadler, and Sayantan Sharma. The topological susceptibility in finite temperature QCD and axion cosmology. *Phys. Lett.*, B762:498–505, 2016.
- [13] Yusuke Taniguchi, Kazuyuki Kanaya, Hiroshi Suzuki, and Takashi Umeda. Topological susceptibility in finite temperature (2+1)-flavor QCD using gradient flow. *Phys. Rev.*, D95(5):054502, 2017.
- [14] Florian Burger, Ernst-Michael Ilgenfritz, Maria Paola Lombardo, Michael Mller-Preussker, and Anton Trunin. Topology (and axion’s properties) from lattice QCD with a dynamical charm. In *26th International Conference on Ultrarelativistic Nucleus-Nucleus Collisions (Quark Matter 2017) Chicago, Illinois, USA, February 6-11, 2017*, 2017.
- [15] J. Frison, R. Kitano, H. Matsufuru, S. Mori, and N. Yamada. Topological susceptibility at high temperature on the lattice. *JHEP*, 09:021, 2016.

- [16] Sz. Borsanyi et al. Calculation of the axion mass based on high-temperature lattice quantum chromodynamics. *Nature*, 539(7627):69–71, 2016.
- [17] B. Berg. Dislocations and Topological Background in the Lattice $O(3)$ σ Model. *Phys. Lett.*, 104B:475–480, 1981.
- [18] Masayuki Asakawa, Tetsuo Hatsuda, Etsuko Itou, Masakiyo Kitazawa, and Hiroshi Suzuki. Thermodynamics of $SU(3)$ gauge theory from gradient flow on the lattice. *Phys. Rev.*, D90(1):011501, 2014. [Erratum: *Phys. Rev.* D92,no.5,059902(2015)].
- [19] Masakiyo Kitazawa, Takumi Iritani, Masayuki Asakawa, Tetsuo Hatsuda, and Hiroshi Suzuki. Equation of State for $SU(3)$ Gauge Theory via the Energy-Momentum Tensor under Gradient Flow. *Phys. Rev.*, D94(11):114512, 2016.
- [20] Simon Caron-Huot, Mikko Laine, and Guy D. Moore. A Way to estimate the heavy quark thermalization rate from the lattice. *JHEP*, 04:053, 2009.
- [21] A. Francis, O. Kaczmarek, M. Laine, T. Neuhaus, and H. Ohno. Nonperturbative estimate of the heavy quark momentum diffusion coefficient. *Phys. Rev.*, D92(11):116003, 2015.
- [22] D.N. Zubarev. *Non-Equilibrium Statistical Thermodynamics*. Pleunum, 1974.
- [23] F. Karsch and H. W. Wyld. Thermal Green’s Functions and Transport Coefficients on the Lattice. *Phys. Rev.*, D35:2518, 1987.
- [24] Harvey B. Meyer. A Calculation of the shear viscosity in $SU(3)$ gluodynamics. *Phys. Rev.*, D76:101701, 2007.
- [25] Harvey B. Meyer. Transport Properties of the Quark-Gluon Plasma: A Lattice QCD Perspective. *Eur. Phys. J.*, A47:86, 2011.
- [26] E.M. Stein and G.L. Weiss. *Introduction to Fourier Analysis on Euclidean Spaces*. Mathematical Series. Princeton University Press, 1971.